JOURNAL OF MATERIALS SCIENCE 8 (1973) 1711–1716

Argon ion etching in a reactive gas

M. CANTAGREL, M. MARCHAL
Thomson-CSF, Laboratoire Central de Recherches, 91401 Orsay, France

It is shown that the sputtering yield of various materials submitted to argon ion (1 keV) bombardment decreases strongly with increase of oxygen pressure in the atmosphere of the sputtering chamber. The sputtering yields are plotted against the "poisoning ratio" (the poisoning ratio is defined as the ratio of the rate of arrival of oxygen molecules at the target surface to that of the rate of removal of sputtered atoms). On the curves representing the sputtering yield versus the poisoning ratio, two particular values are pointed out for each material. Between these two values the sputtering yield decreases as the poisoning ratio increases, out of these values the sputtering yield is quite independent of the poisoning ratio.

In the region of high poisoning ratio value, the spread of the sputtering yield for investigated materials is wider than in the region of low poisoning ratio value. Thus, we observed, in terms of etching rate, a ratio of 7 between silica and chromium and a ratio of 10 between silica and vanadium when the oxygen pressure introduced in the target chamber is 10^{-4} Torr. These results are used in order to obtain deep grooves in silica, when such metals are used as masking materials.

New data on the sputtering yield of various materials is provided.

1. Introduction

Several investigators [1-4] have shown that the sputtering yield of aluminium and silicon is significantly reduced when these materials are bombarded with argon ions in an oxygen atmosphere. On the other hand, the sputtering yield of silica, alumina and copper seems to be only slightly affected under the same conditions.

We report in this paper new data on the sputtering yields of metals and oxides subjected to argon ion bombardment in the presence of oxygen. In particular we have observed that the sputtering yields and the etching rates of materials could be related to the oxygen partial pressure in the target chamber. These results are discussed using the so called "poisoning ratio" introduced by Andrews [1].

By association of two materials suitably chosen regarding their respective etching rate towards oxygen partial pressure, it becomes possible to realize deep grooves by ion etching using a thin, high definition metallic mask. This is of special interest for the realization of waveguides used in integrated optics.

2. Experimental technique and procedure

The experimental apparatus illustrated in Fig. 1 consists of two vacuum chambers. The upper one is the ion gun ionization chamber, the lower one is the target chamber. This ion gun was developed from the basic design of the Kaufman source [5]. A cylindrical anode accelerates electrons emitted from a hot filament. The ionization of a 7×10^{-4} Torr argon atmosphere is enhanced by a magnetic coil. Ions are extracted through three grids having matching arrays consisting of 370 holes, each of which is 3 mm in diameter. This results in an ion beam uniform to within 5% over a 40 mm diameter area. The ion density can be varied from 0.3 to 2 mA cm^{-2} as the accelerating voltage is adjusted from 0.5 to 2 kV. A charge-compensating filament emits electrons into the ion beam in order to avoid charge build up when insulators are etched.

Samples are bonded onto a water-cooled target holder using a silicon grease film to ensure thermal contact.

© 1973 Chapman and Hall Ltd.

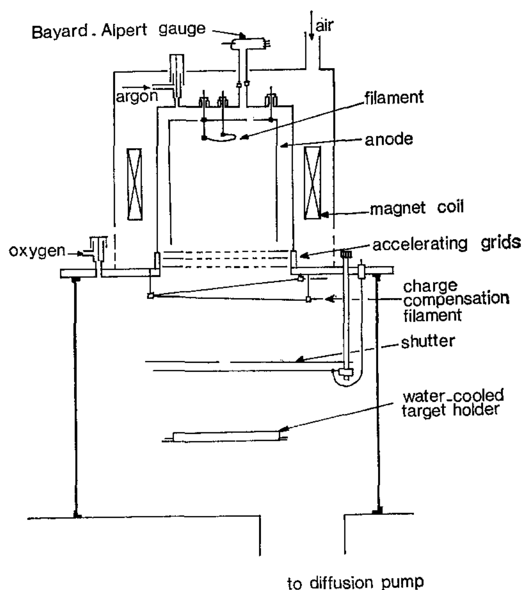

Figure 1 Ion micro-etching machine.

A standard process was chosen for all experiments.

The whole apparatus is pumped down until 3×10^{-7} Torr residual gas pressure is reached. This value is approximately the background pressure limit of the vacuum station.

While pumping is kept on, oxygen is introduced in the target chamber through a leak valve. The pressure is measured with a nitrogen calibrated Bayart Alpert gauge.

Argon is then introduced in the ionization chamber up to 7×10^{-4} Torr pressure.

The ion gun is turned on, the ion energy is adjusted to 1 keV and the resulting ion current density is 0.6 mA cm^{-2}.

The shutter is removed when the ion beam is in a steady state.

Etching rates and sputtering yields are calculated from the depth of steps ion etched through either a photoresist or metallic mask. Depths are measured using a stylus instrument (Talystep).

3. Effect of oxygen partial pressure on etching rates and sputtering yields

Etching rates and sputtering yields have been measured:

(1) As a function of the oxygen partial pressure in the range 10^{-4} Torr to 5×10^{-6} Torr. This last value is the lowest that can be accurately controlled with our equipment. The upper value is limited by the operating argon pressure in the ionization chamber.

(2) As a function of the residual pressure in the target chamber in the range 10^{-6} Torr to 3×10^{-7} Torr without any introduction of oxygen.

Targets used for all these measurements were high purity aluminium, silicon and silica, evaporated aluminium and manganese thin films and sputtered vanadium and chromium thin films.

TABLE I Sputtering yield of various materials

	S (at. or mol/ion) *E* = 1 keV	*S* [6] *E* = 600 eV	*S* [7] *E* = 1 keV
Aluminium			
bulk	1.3	1.2	
thin film	0.7		
Chromium			
bulk		1.3	
thin film	0.85		
Manganese			
bulk	1.1		
thin film	0.65		
Molybdenum			
bulk		0.9	1.1
thin film	0.9		
Silica (fused)			
bulk	0.26		0.13
Silicon			
bulk	0.6	0.5	0.6
Tantalum			
bulk	0.65	0.6	
Titanium			
bulk	0.52	0.6	
thin film	0.3		
Vanadium			
bulk		0.7	
thin film	0.4		
Corundum			
bulk	0.08		0.04

3.1. Sputtering yields measured at 3×10^{-7} Torr residual pressure

Table I lists the measured values of the sputtering yields. It can be noticed that measured sputtering yields on bulk materials are in good agreement with published data [6, 7]. On the contrary the values observed with thin films are always smaller than the values observed for corresponding bulk material. This difference may be attributed to the higher impurity content of the thin films.

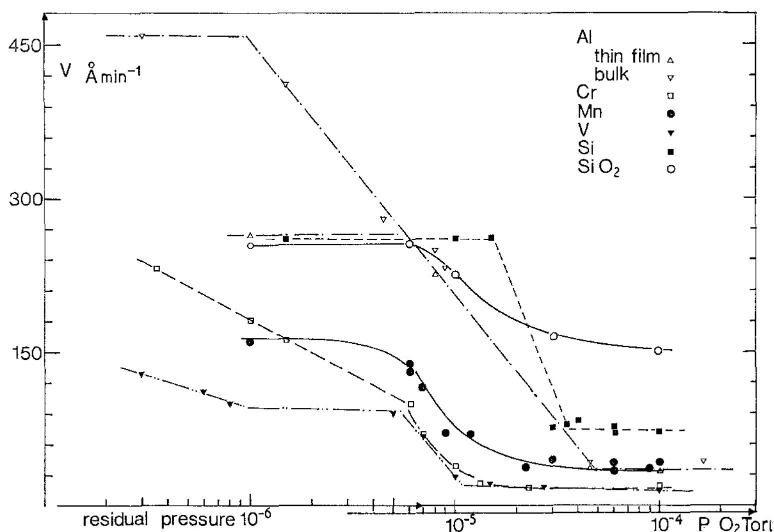

Figure 2 Al, Cr, Mn, V, Si, SiO_2 milling rate as a function of oxygen pressure.

3.2. Sputtering yields and etching rates as a function of oxygen partial pressure

The etching rate versus oxygen pressure curve exhibits the same shape for all the materials studied as shown by Fig. 2. The typical curve can be divided into three parts with regard to the oxygen partial pressure. With increasing oxygen pressure, we find a first plateau where the etching rate is quite independent of oxygen partial pressure or residual gas pressure. This first plateau is followed by an intermediate region where the etching rate decreases rapidly as oxygen pressure increases. Then a second plateau corresponds to a new oxygen pressure-independent etching-rate region.

All materials investigated exhibit a decrease of etching rate as oxygen partial pressure increases. The ratio between etching rates at low oxygen partial pressure and at high oxygen partial pressure is different for each material. Silica has a low ratio: 1.7 whereas the highest ratio which is found for bulk aluminium, reaches 11.

The pressure limits of the intermediate region are also different for different materials. For example the oxygen pressure limits are for silicon 1.5×10^{-5} Torr to 4×10^{-5} Torr and for chromium 7×10^{-6} Torr to 1.2×10^{-5} Torr. So while chromium has reached its lowest etching rate plateau, silicon is still in the highest etching rate plateau. The ratio of etching rates between silicon and chromium reaches a values of 12 at 1.5×10^{-5} Torr oxygen partial pressure .

A first application of these results is the ion etching of optical waveguides for integrated optics. For our application the substrate was silica. In order to obtain a given depth for the waveguide, the etching rate of silica is to be compared to that of potential mask materials at the same oxygen partial pressure. From the curves of Fig. 3, at 10^{-4} Torr oxygen partial pressure the etching rate ratio between silica and chromium is 7, and, at the same oxygen pressure this ratio is 10 between silica and vanadium. Without the use of oxygen, these ratios would be 1.1 and 2 respectively. The highest observed ratio is 3 between silica and carbon under the same conditions.

3.3 Discussion

The sputtering yields of the materials studied can be related to the "poisoning ratio". The poisoning ratio, introduced first by Andrews and co-workers [1], is defined as the ratio of the rate of arrival of oxygen molecules at the target surface to the rate of removal of sputtered material from the surface. The poisoning ratio R is given by:

$$R = \frac{5.8 \times 10^7 \times P}{I \times S}$$

where P is oxygen pressure in Torr; I is ion current density in $\mu A\ cm^{-2}$ and S is the sputtering yield.

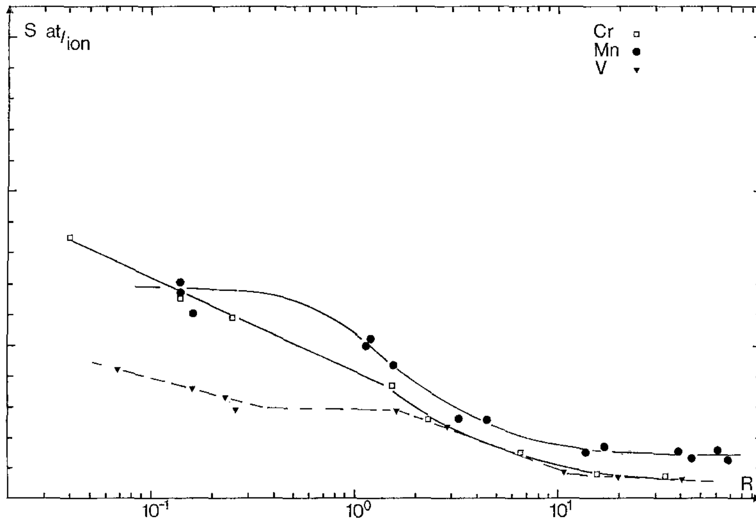

Figure 3 Cr, Mn, V, sputtering yield as a function of the poisoning ratio.

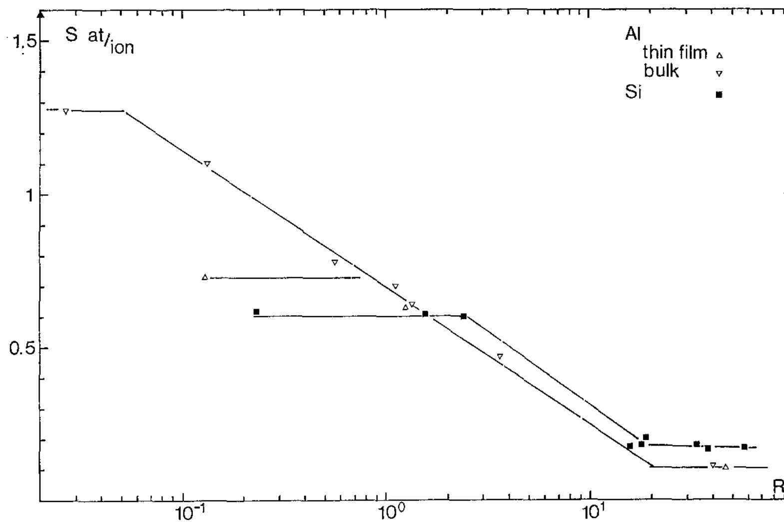

Figure 4 Al, Si, sputtering yield as a function of the poisoning ratio.

Figs. 3 and 4 show the sputtering yields of chromium, manganese, vanadium, aluminium and silicon as a function of the poisoning ratio. It should be noticed that the rapid decrease of sputtering yields takes place within a narrow range of poisoning ratio values for all materials studied, this range being 0.1 to 10.

An explanation of such a variation of sputtering yield as a function of the poisoning ratio may be proposed. The oxygen molecules colliding with the sample are trapped on its surface. In the case of the materials investigated, the trapped oxygen is chemisorbed. This chemisorbed oxygen is sputtered from the surface in the same way as it will be from an oxide surface. When the poisoning ratio increases, the oxygen coverage increases and the sputtering yield of the material reaches the sputtering yield of the oxidized material. This is well verified on silicon and silica. Measured sputtering yield at 10^{-4} Torr oxygen pressure is 0.17 for silicon and 0.15 for silica (measured in molecules/ion). That is,

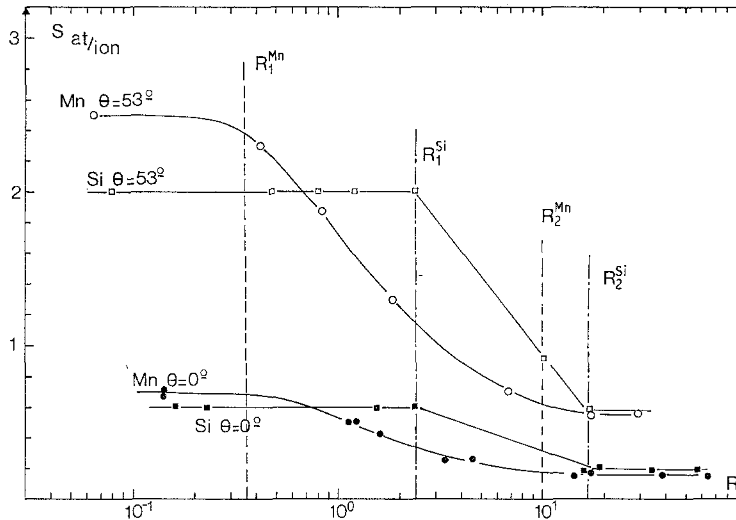

Figure 5 Sputtering yield as a function of poisoning ratio and angle of incidence.

the sputtering yield of silicon atom from silicon or silica targets is similar. This observation has already been reported by Blanchard [4] who observed that the ionic emission of Si^+ was the same for silicon and silica in similar conditions.

A decrease of the etching rate of silica occurs when the oxygen pressure is increased. Hasseltine [2] observed a similar phenomena with alumina. He explained this fact as a replacement of sputtered oxygen atoms by atoms of oxygen from the environment, while the corresponding silicon atom is not sputtered. So comparisons between a material and its oxide must be made under the same ion etching conditions.

In order to test the validity of the concept of the poisoning ratio throughout the oxygen pressure range, ion etching conditions have been varied. Ion density and sputtering yield have been changed while ion energy remained constant.

Fig. 5 shows the sputtering yield of silicon and managanese as a function of the poisoning ratio for two values of the angle of incidence. We notice that the values of the poisoning ratio which limit the rapid change of the sputtering yield, remain the same for a given material although the sputtering yield and the current density are changed due to the variation of incidence. So two "intrinsic" values of the poisoning ratio are found for each material. These intrinsic values are 2.5 and 18 for silicon and 0.35 and 10 for manganese. This result enables us to calculate the two oxygen pressure limits for the intermediate region of the etching rate versus oxygen pressure curve when experimental conditions are changed.

4. Application to the ion etching of optical waveguides

All these measurements were made in order to provide basic data for further choice of a masking material which may be used to obtain grooves of sufficient depth to be usable as an optical waveguide. The minimum acceptable depth is 0.6 μm in silica owing to the wavelength of the light used.

The typical process described in Fig. 6 is known as the lift off technique [8]. The main steps are as follows:

(1) A 0.5 μm thick film of PMM is spin-coated onto the substrate (a).

(2) The PMM is exposed by the electron beam of a scanning electron microscope (b).

(3) The PMM is developed (c).

(4) A 2500 Å metallic film is deposited on the substrate (d).

(5) The remaining PMM and unwanted metallic film are removed.

(6) The sample is argon ion etched at a suitable oxygen partial pressure (e).

(7) The remaining metallic film is removed (f).

Fig. 7 is a scanning electron microscope photograph of a waveguide obtained with a 2500Å

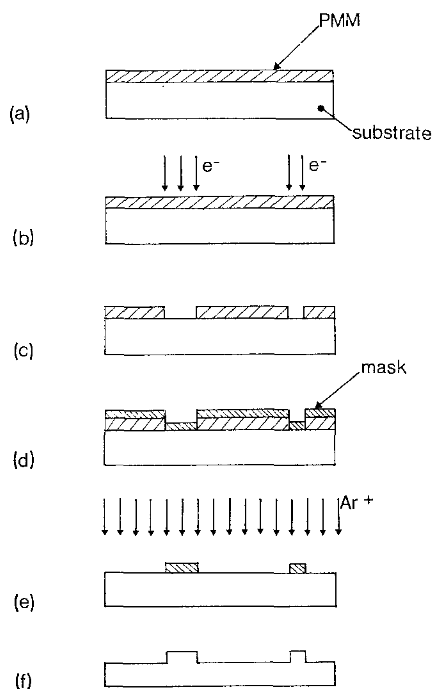

Figure 6 Main steps of ion-etched pattern process.

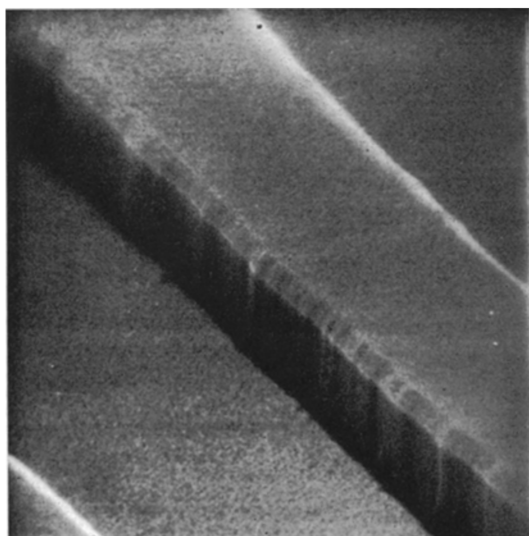

Figure 7 Grooves ion etched in silica. A part of the chromium mask remains on the protected part of the pattern (× 25000).

thick chromium mask. Its dimensions are 1.2 μm in depth and 2.2 μm in width.

5. Conclusions

Etching rates and sputtering yields of a variety of materials were measured as a function of the oxygen partial pressure in the target chamber.

The variation of the etching rate and sputtering yield can be related to the ion density and the oxygen partial pressure through the term of poisoning ratio. Two intrinsic values of the poisoning ratio were pointed out, for silicon and manganese. Between these values the sputtering yield decreases as the poisoning ratio increases. Outside these values the sputtering yield is quite independent of the poisoning ratio.

The extent to which the etching rate decreases is different for different materials. It is possible to take advantage of this etching-rate reduction for the ion etching of an optical waveguide. Deep grooves up to 1.2 μm depth have been obtained in silica using 2500 Å chromium mask.

References

1. A. E. ANDREWS, E. H. HASSELTINE, N. T. OLSON and H. P. SMITH Jun., *J.Appl. Phys.* **37** (1966) 3344.
2. E. H. HASSELTINE, F. C. HULBURT, N. T. OLSON and H. P. SMITH Jun., *ibid* **38**(1967) 4313.
3. J. F. HENNEQUIN, *C.R. Acad. Sc.* **264** *série B* (1967) 1127.
4. B. BLANCHARD, N. HILLERET and J. MONIER, *Mat. Res. Bull.* **6** (1971) 1283.
5. H. R. KAUFMAN and P. D. READER, in "Electrostatic propulsion" (edited by D. B. Langmuir, E. Stuhlinger and J. M. Sellen Jun.) (Academic Press, New York, 1961).
6. N. LAEGRIED and G. K. WEHNER, *J. Appl. Phys.* **32** (1961) 365.
7. L. I. MAISSEL and R. GLANG, "Handbook of thin film technology" (McGraw Hill, 1970) pp. 4-40.
8. I. HALLER, M. HATZAKIS and R. SRINIVASAN, *IBM J. Res. Develop.* **12** (1968) 251.

Received 4 June and accepted 19 June 1973.